Desalination and Water Treatment
www.deswater.com

doi: 10.1080/19443994.2015.1054311

57 (2016) 11820–11834
May

Taylor & Francis
Taylor & Francis Group

Adsorptive removal of phenol from aqueous solutions by copper (cu)-modified scoria powder: process modeling and kinetic evaluation

Masoud Moradi[a,b], Amir Mohammad Mansouri[a,c], Nahid Azizi[d], Jila Amini[d], Kaveh Karimi[d], Kiomars Sharafi[d,e,*]

[a]*Research Center for Environmental Determination of Health (RCEDH), Kermanshah University of Medical Sciences, Kermanshah, Iran, emails: Mahfooz60@gmail.com (M. Moradi), amansouri.mansouri84@gmail.com (A.M. Mansouri)*
[b]*Environmental Health Engineering, Iran University of Medical Sciences, Tehran, Iran*
[c]*Faculty of Chemistry, Department of Analytical Chemistry, Razi University, Kermanshah, Iran*
[d]*Department of Environmental Health Engineering, Kermanshah University of Medical Sciences, Kermanshah, Iran, emails: azizi_nahid92@yahoo.com (N. Azizi), jilaamini1@gmail.com (J. Amini), karimik6@gmail.com (K. Karimi), Kio.sharafi@gmail.com (K. Sharafi)*
[e]*Department of Environmental Health Engineering, Tehran University of Medical Sciences, Tehran, Iran*

Received 15 June 2014; Accepted 20 April 2015

ABSTRACT

Phenol compounds are regarded as hazardous pollutants due to their toxicity and carcinogenic properties to human health at low concentrations. So, this study was aimed to investigate the phenol adsorption by copper (Cu)-modified scoria powder, which is a low-cost adsorbent for the removal of organic compounds. All the experiments were performed based on the full face-centered central composite design experimental plan and analyzed using response surface methodology. The samples were analyzed using various conditions including adsorbent dose (0.1–1 g/l), phenol concentration (50–250 mg/l), and contact time (5–100 min). Three-dimensional plots reveal the relationship between the phenol removal efficiency and the paired factors, which describe the behavior of scoria powder in the removal of phenol from aqueous solution. The models showed that phenol removal efficiency in aqueous solution affected by four studied factors. A maximum removal efficiency of phenol achieved was more than 96% at the optimum conditions (scoria dosage of 1 g/l, phenol concentration of 50 mg/l, and contact time of 100 min). Process of kinetic parameters were also evaluated and modeled using five kinetic models including pseudo-first-order equation, second-order equation, modified Freundlich, pore diffusion, and Elovich. The best fit of experimental adsorption data was calculated by means of the pseudo-second-order model. Equilibrium data obeyed the Freundlich and Langmuir isotherms, and found that the equilibrium data well obeyed the Langmuir isotherm.

Keywords: Adsorptive removal; Phenol; Aqueous solutions; Scoria powder

*Corresponding author.

1. Introduction

Phenol compounds are nonpolar and hydrophobic in nature; their aqueous solubility limits are significantly higher than the level of maximum contaminants and they are common contaminants in wastewater generated from oil refineries, coal conversion plants, petrochemicals, polymeric resins, coal tar distillation, pharmaceuticals, etc. [1,2]. These compounds are considered because of their potential toxicity to human health organisms such as kidney, central nervous system, liver, and pancreas [3,4]. Due to their toxicity and carcinogenic properties to human health at low concentrations, they have been classified as hazardous pollutants. The regulations of US Environmental Protection Agency and Institute of Standards and Industrial Research of Iran have called for lowering phenol content in wastewater to less than 1 and 0.5 μg/l, respectively [5,6]. Therefore, to achieve the maximum allowable levels of pollutants according to health and environmental instructions, it is recommended to remove phenol from industrial effluents before entering the aqueous solution [7,8].

Various processes have been employed for the removal of phenols from aqueous media which include ozonation [9], wet air oxidation [10], advanced oxidation [11], wet peroxide oxidation [12], biological and photocatalytic degradation [13,14], and adsorption [15]. However, chemical methods of pollutant removal lead to producing a large amount of sludge, which can create disposal problems. Furthermore, these methods need chemicals and electrical energy, which further pose problems for the environment. Among these methods, adsorption seems to be one of the economical and most effective methods because of its simple operation and easy handling. High cost for the removal of pollutants from aqueous solutions using adsorption on commercial activated carbons, though very effective, has motivated the search for alternative adsorbents [4]. Scoria is a vesicular (bubbly) glassy lava rock of basaltic to andesitic composition which is ejected from a vent during explosive eruption. The bubbly nature of scoria is due to the escape of volcanic gasses during eruption. Scoria is typically dark gray to black in color, mostly due to its high iron content. Because of its microporous structure and high specific surface area. Recently, many researchers have used scoria for the removal of cadmium, disinfection byproduct, heavy metals, and sulfur dioxide [16–19]. Since initial scoria has some impurity, it shows low sorption capacity and is also negatively charged [20]; so, to increase the efficiency (as a new adsorbent), some methods such as acidic treatment, metal coating, thermal activation, etc. are used [3,21] Therefore, the purpose of scoria modified with metals such as copper is to improve the positive surface charge of adsorbent and improve its sorption capacity for more removal of pollutants in order to set the maximum allowable levels.

Response surface methodology (RSM) is a collection of mathematical and statistical techniques which are useful for analyzing the effects of several independent variables on the response [22]. RSM has an important application in the process analysis and optimization as well as the improvement of the existing design. This methodology is practical, since it is taken from experimental methodology which includes interactive effects among the variables and, eventually, depicts the overall effects of the parameters on the process [23]. In the last few years, RSM has been applied to optimize and evaluate interactive effects of independent factors in numerous chemical and biochemical processes [24–26].

Furthermore, the conventional technique for the optimization of a multi-factorial system is to deal with one factor at a time. However, this type of method is time consuming and also does not reveal the alternative effects among components. Therefore, in this work, the central composite design (CCD) was applied for the modeling and optimization of adsorptive phenol removal from aqueous solutions by copper (Cu)-modified scoria powder (CSP) in order to estimate the interactions among the variables as well as their direct impacts on the process. Furthermore, most of the studies on the adsorption of phenol by different adsorbents have not been in-depth about the adsorption kinetics, which is also important scientific information; hence, this study also investigated the kinetics of phenol adsorption by CSP in order to develop the kinetic equations which can provide fundamental knowledge for future use. Thus, the main objectives of this work was as follows: (1) to obtain experimental equilibrium data; (2) to determine a suitable model for describing the isotherms; (3) to determine kinetic parameters of phenol adsorption on CSP; and (4) to estimate the interactions among the three variables (CSP dosage, phenol concentration, and contact time) as well as their direct impacts on the process.

2. Materials and methods

2.1. Preparation of CSP

Scoria stone was sieved and particles were kept in 1% HCl for 24 h and washed for several times with deionized water in order to remove the impurity of scoria stone. The particles were then dried in an oven at 105°C for 14 h. These fractions were coated with

copper as follows: 50 g of scoria particles and 150 mL of 0.01 M $CuSO_4$ solution were added to a beaker and pH was adjusted to 8.5 by adding 0.1 M NaOH solution. Thereafter, the beaker was placed on a shaker at laboratory temperature (25 ± 1˚C) for72 h and then the obtained material was dried at 105˚C in the oven for 24 h as well. In order to remove the traces of uncoated $CuSO_4$ from the particles, the dried particles were washed again with double-distilled water and dried in the oven at 105˚C for 24 h [27].

2.2. Analysis and data calculation

A Fourier transformed infrared (FTIR) spectrometer (ABB BOMEM MB 104 SERIES, SWIS) in the transmittance mode at 50 scans with the resolution of 4 cm^{-1} in the frequency range of 800–4,000 cm^{-1} was used to analyze the FTIR spectra of the samples as pressed pellets in KBr. The chemical characteristics of the scoria samples were determined by an XRF (Shimadzu XRF-6000). Surface morphology of the scoria powder was studied by scanning electron microscopy using a Philips XL30 microscope at the accelerating voltage of 10 kV. After the oven drying of the scoria powder for 12 h, the sample was coated with a platinum layer using an SCDOOS sputter coater (BAL-TEC, Sweden) in an argon atmosphere. Subsequently, the sample was scanned and photomicrographs were obtained. Stock solution of phenol of 1,000 ppm was prepared and diluted to the required initial concentrations. Distilled water was employed for preparing the phenol solutions. The adsorption of phenol from aqueous solution onto CSP was performed using batch equilibrium technique. For the phenol determination, the samples were centrifuged at 2,000 rpm for 15 min and the remaining concentration in the supernatant solution was analyzed using UV–visible spectrometry (Hitachi Model 100-40) at the appropriate wavelength corresponding to the maximum absorbance of phenol: 270 nm.

2.3. Batch-mode sorption studies

All the experiments were conducted in the batch mode in various conditions in terms of adsorbate initial solutions of phenol (50–250 mg/l), adsorbent dose (0.1–1 g/l), pH (3–11), contacted time (20–100 min), and temperature (20–50˚C). Adsorption experiments were carried out in 500 ml Erlenmeyer flasks by five different concentrations of phenol and adsorbent. A certain amount of scoria powder was mixed with 100 ml of phenol solution by rotary mixer (H1-190 M) at 150 rpm according to the experimental design. Then, the slurry samples were centrifuged at 4,000 rpm for 10 min to remove adsorbent and then concentration of the residual phenol in aqueous solutions was analyzed by spectrophotometer (Hitachi Model 100-40) at appropriate wavelength corresponding to the maximum absorbance: 270 nm [28].

The adsorption capacity of CSP was calculated using equilibrium studies. The mass balance equation for this process at equilibrium condition is given by

$$q_e = \frac{(C_0 - C_e)V}{M} \quad (1)$$

where q (mg/g) is the adsorbent capacity, C_0 (mg/l) is the initial concentration of phenol, Ce (mg/l) is the final or equilibrium concentration of phenol, V is the experimental solution volume (l), and M is the weight of CSP (g).

2.4. Experimental design

The statistical method of factorial design of experiments (DOE) eliminates systematic errors with an estimate of the experimental error and minimizes the number of experiments [29–31]. The RSM used in the present study was a central composite face-centered design (CCFD) involving four different factors of CSP dosage, contact time, pH, and phenol concentration. The range studied for the CSP dosage, phenol concentration, contact time, and pH is presented in Table 1. The removal efficiency CSP was assessed based on the full face-centered CCD experimental plan (Table 2). The design consisted of $2k$ factorial points augmented by $2k$ axial points and a center point where k is the number of variables. The four operating variables were considered at five levels: $-\alpha(-1.5)$, −1, 0, 1, and 1.5, and assessed based on the full face-centered CCD experimental plan. Accordingly, 30 experiments ($=2k + 2k + 6$, where k is the number of factors) were conducted with 25 experiments organized in a factorial design (including 16 factorial points, 8 axial points, and 1 center point) and the remaining 5 involved the replication of the central point to get a good estimate of the experimental error. Repetition experiments were carried out followed by the order of runs designed by DOE, as shown in Table 2.

2.5. Mathematical modeling

After conducting the experiments, the coefficients of the polynomial model were calculated using the following equation [29]:

Table 1
Experimental range and level of the independent variables

	Range and level				
Variables	−α (−1.5)	−1	0	1	+α (1.5)
Contact time (min)	20	40	60	80	100
Adsorbent dosage (g/l)	0.2	0.4	0.6	0.8	1
pH	3	5	7	9	11
Phenol concentration (mg/l)	50	100	150	200	250

Table 2
Experimental conditions and results of CCD

	Variables				Response (phenol removal by scoria-Cu)	
Run	Factor 1 A: Scoria dosage (g/l)	Factor 2 B: Contact time(min)	Factor 3 C: pH	Factor 4 D: Phenol concentration (mg/l)	Actual %	Predicted %
1	0.2	20	3	250	46.58	48.12
2	0.8	60	7	150	74.60	68.97
3	0.2	20	11	50	9.34	11.44
4	0.6	60	7	150	62.86	67.69
5	1	20	3	50	85.21	86.74
6	1	100	11	50	32.65	31.84
7	1	20	11	250	12.15	14.57
8	0.6	80	7	150	75.35	68.97
9	0.6	60	7	200	65.56	62.65
10	1	100	3	250	72.29	70.92
11	0.2	100	3	250	56.27	57.81
12	1	20	11	50	25.74	23.69
13	0.2	100	11	250	11.86	11.05
14	1	20	3	250	62.72	60.85
15	0.6	40	7	150	61.70	64.51
16	0.2	100	3	50	84.44	82.75
17	0.6	60	7	150	69.90	67.69
18	0.6	60	5	150	78.43	79.29
19	0.4	60	7	150	60.57	62.63
20	0.2	20	11	250	8.14	5.41
21	1	100	11	250	18.29	20.58
22	0.6	60	7	150	64.40	67.69
23	0.6	60	7	150	68.55	67.69
24	0.6	60	7	100	71.84	71.17
25	0.6	60	7	150	61.90	67.69
26	1	100	3	50	96.71	98.94
27	0.6	60	7	150	65.12	67.69
28	0.6	60	9	150	56.28	51.84
29	0.2	100	11	50	17.85	19.22
30	0.2	20	3	50	73.71	70.92

$$Y = \beta_0 + \beta_i X_i + \beta_j X_j + \beta_{ii} X_i^2 + \beta_{jj} X_j^2 + \beta_{ij} X_i X_j + \ldots \quad (2)$$

where i and j are the linear and quadratic coefficients, respectively, and β is the regression coefficient.

The model terms were selected or rejected based on the p value with 95% confidence level. The results were completely analyzed using Analysis of Variance (ANOVA) by Design Expert software. Three-dimensional plots and their respective contour plots were obtained

based on the effect of the levels of the three factors. Using these three-dimensional plots, the simultaneous interaction of the three factors on the response was studied. The experimental conditions and results are shown in Table 2.

3. Results and discussion

3.1. Scoria characterization

Natural scoria samples were obtained from Ghorve, Kurdistan Province, Iran, and had the bulk density of 0.67 g cm^{-3}. The chemical composition of scoria powder samples was characterized by XRF. The results showed the composition of SiO_2 (67%), Al_2O_3 (15.6%), K_2O (5.4%), Fe_2O_3 (1.1%), Na_2O (3.7%), CaO (2.9%), MgO (0.2%), etc. As seen from the values, the two most important components of the sample were SiO_2 and Al_2O_3. It can be concluded that the higher the silica percentage, the purer the scoria would be. Moreover, high iron oxide content not only darkened the color of the scoria, but also increased its density. FTIR spectrum is the feature of a particular compound that gives information about its functional groups, molecular geometry, and inter/intermolecular interactions. Fig. 1 shows the FTIR spectra of scoria powder. The strong peak around 1,033 cm^{-1} may have been resulted from Si–O stretching vibrations [32]. The other important peak was detected around 3,450 cm^{-1} and pointed out the OH stretching vibrations of water (moisture) which was adsorbed by the sample from the outside environment [33]. The relatively strong peak around 1,635 cm^{-1} was probably resulted from the carboxyl group stretching vibrations [32]. SEM images showing the details of the microstructure (that is, inner pore structure) of the scoria are displayed in Fig. 2. According to the SEM images, the scoria sample had irregular or oval shape and fibrous cavities (or pores); in addition, it may be said that these pores were either in closed or in open forms. The pore diameter of these cavities varied between 1 and 30 μm and these cavities generally did not intersect each other.

3.2. Effect of CSP dose

To find the optimum amount of CSP dose, which can completely remove phenol from aqueous solution, a batch-mode sorption study was performed using various amounts of CSP dose. Fig. 3 shows the

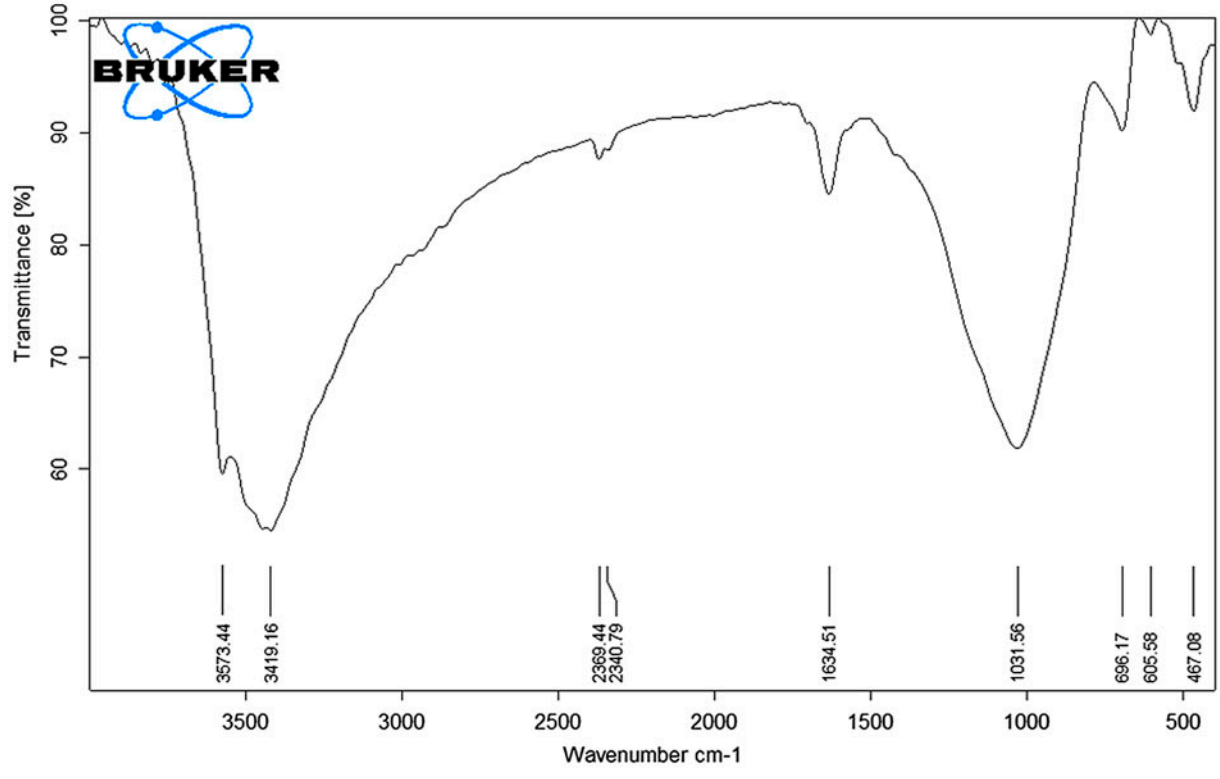

Fig. 1. FTIR spectrum of CSP.

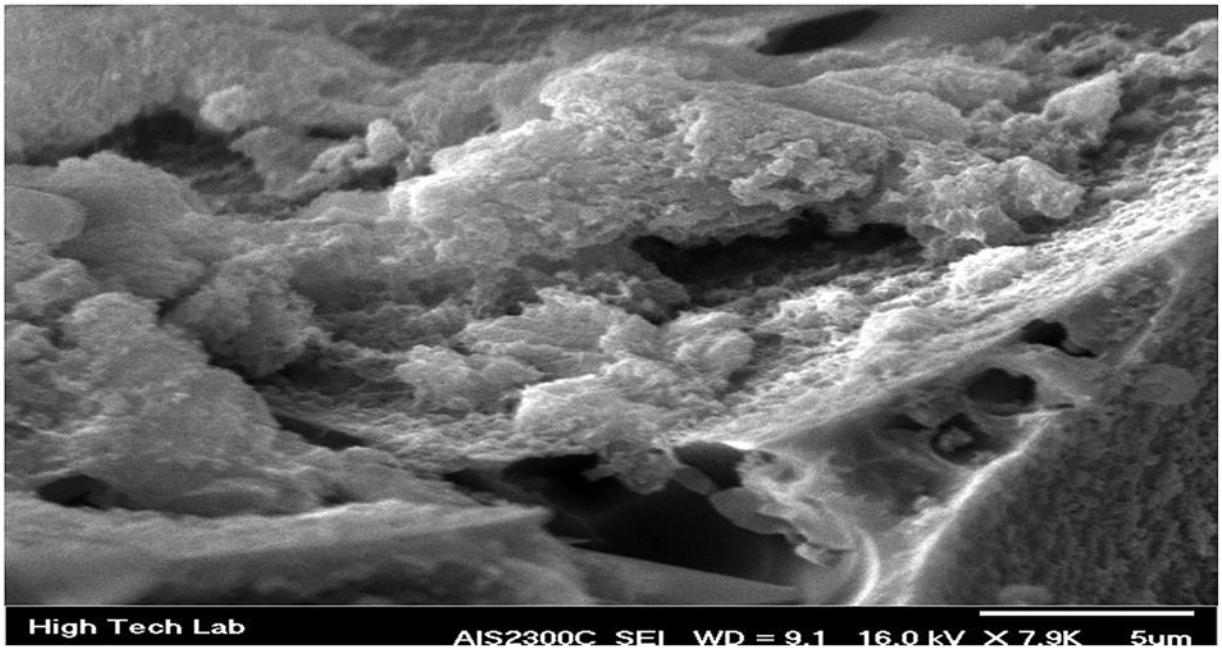

Fig. 2. SEM image of CSP sample.

removal of phenol as a function of CSP dosage. In general, an increase in CSP dosage increased the percent removal of phenol. In order to remove phenol quantitatively from the aqueous solution, the optimum amount of CSP was found as 1 g/l and phenol solution (50 mg/l).

3.3. Equilibrium study

Equilibrium sorption isotherm is used to describe adsorbent capacity and is one of the important parameters for adsorption system designing [34,35]. Seeking the best model among different isotherm models is of principle significance for the process

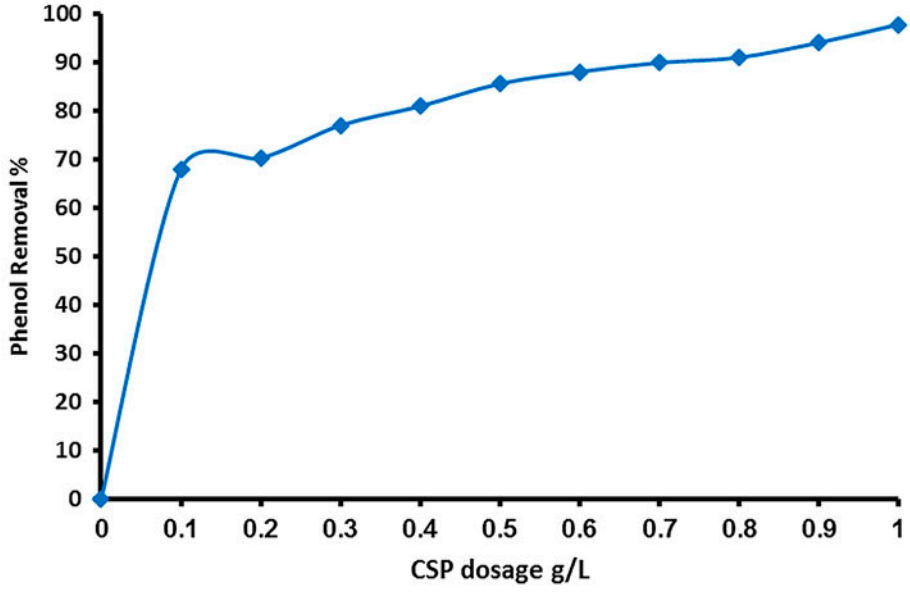

Fig. 3. Effect of CSP dosage on the removal of phenol from aqueous solution.

design as well as for the improvement of knowledge on the adsorption mechanism [36]. In the present investigation, the equilibrium adsorption data were analyzed according to the linear form of the Langmuir (Eq. (3)) and Freundlich (Eq. (4)) isotherm models.

$$\frac{1}{q_e} = \frac{1}{q_0} + \frac{1}{bq_0C_e} \tag{3}$$

where C_e is the equilibrium concentration (mg/l), $q_e$is the amount adsorbed at equilibrium (mg/g), and q_0 and b are the Langmuir constants related to the capacity and energy of adsorption, respectively.

The Langmuir adsorption isotherm plot ($1/q_e$ vs. $1/C_e$) (Fig. 4(a)) indicated the applicability of Langmuir adsorption isotherm. The values of q_0 and b were calculated from the slope and intercept of the linear plots $1/q_e$ vs. $1/C_e$ (Table 3). The experimental results indicated the maximum uptake value (q_0) of 43.47 mg phenol per g dry scoria and energy of sorption value (b) of 0.035 mg^{-1}.

A dimensionless constant separation factor, R_L, was defined to assess the validity of the Langmuir-type adsorption process [37].

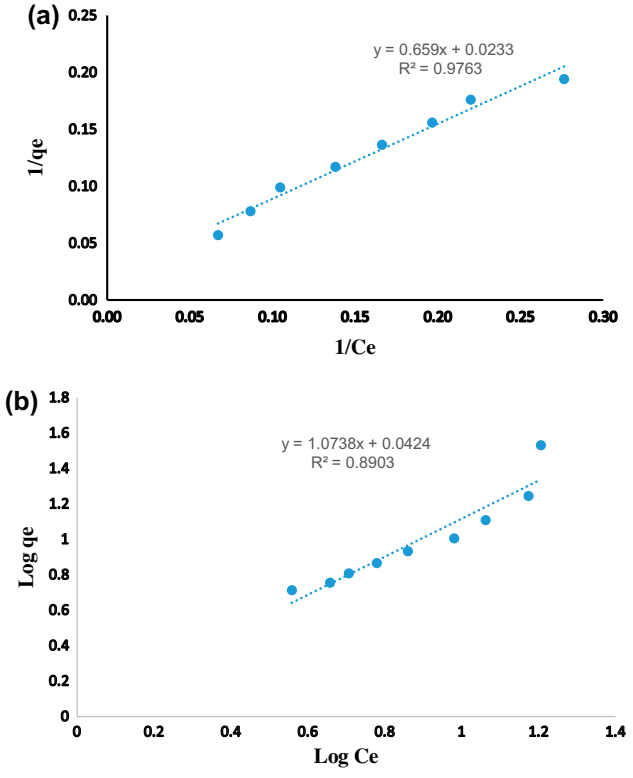

Fig. 4. Isotherm plots for the adsorption of phenol onto CSP. (a) Langmuir isotherm and (b) Freundlich isotherm.

$$R_L = \frac{1}{1 + bC_0} \tag{4}$$

where C_0 is the initial concentration and b is the Langmuir isotherm constant. The value of R_L determines whether the isotherm is irreversible ($R_L = 0$), favorable ($0 < R_L < 1$), linear ($R_L = 1$) or unfavorable ($R_L > 1$).

The values of R_L for the initial concentration of phenol (50–250 mg/l) were found to be in the range of 0.13–0.36, indicating that the adsorption of phenol onto adsorbent was favorable.

The commonly used Freundlich isotherm model is given by:

$$\log q_e = \log K_f + \frac{1}{n}\log C_e \tag{5}$$

where K_f and $1/n$ are Freundlich constants related to adsorption capacity and adsorption intensity, respectively [38–41].

The Freundlich isotherm model describes adsorption on a heterogeneous surface and is not restricted to monolayer formation. Fig. 4(b) shows that predicted equilibrium adsorption values using Freundlich isotherm model and the good fit to experimental equilibrium adsorption data. The values of K_f and $1/n$ calculated from the intercept and slope of the plot of log q_e vs. log C_e are listed in Table 3. In general, as K_f value increased, the adsorption capacity of the adsorbent was increased. The values of K_f and n were found to be 1.1 (mg/g $(L/mg)^{1/n}$) and 0.932, respectively. For these adsorption processes, phenol adsorption onto CSP at 20°C represented beneficial adsorption. The Langmuir model also gave a satisfactory correlation coefficient ($r^2 = 0.976$) and average percentage error (APE) of 0.05%; however, the correlation coefficient and APE

Table 3
Isotherm equation parameters for phenol adsorption on CSP

Langmuir isotherm	
q_o (mg/g)	43.47
b	0.35
r^2	0.97
APE (%)	0.05
Freundlich isotherm	
n_T	0.932
K_f (mg/g$(L/mg)^{1/n}$)	1. 1
r^2	0. 89
APE (%)	0.5

error for Langmuir model were, respectively, higher and lower than those obtained by means of the Freundlich model ($r^2 = 0.89$ and APE = 0.5%). Hence, the sorption of phenol on CSP followed Langmuir isotherm.

3.4. Kinetic study

Kinetic studies were used to investigate the sorption mechanism and its rate controlling steps, which contain transport and chemical reaction processes [42].

The kinetic behavior of this process was studied at 20°C using four different initial phenol concentrations (Fig. 5). It appears in Fig. 5 that the kinetics of phenol adsorption consists of two phases: an initial rapid phase when the process is very fast and a second slower phase when it reaches equilibrium. The initial high rate of phenol uptake was probably due to the greater availability of binding sites near the surface of the CSP and, after a lapse of time, the remaining vacant surface sites were difficult to be occupied due to repulsive forces between the solute molecules on the solid and bulk phases. Adsorption capacity increased with an increase in the initial phenol concentration, but the time required to reach equilibrium was independent from the initial phenol concentration.

According to Fig. 5(a), with increase in the dose of sorbent, the uptake capacity of phenol per unit mass of sorbent (q, mg/g) was decreased, while the removal percentage of dye was increased. The primary factor for explaining these characteristics is that, during the adsorption process, the number of sites available for adsorption increases by increasing the adsorbent dose.

(1) In order to study the controlling mechanisms of the adsorption process, pseudo-first-order (Eq. (6)), pseudo-second-order (Eq. (7)), intra-particle diffusion (Eq. (8)), modified Freundlich (Eq. (9)), and Elovich (Eq. (10)) equation models were used to test the experimental kinetic data.

(2) Pseudo-first-order model:

$$\log\left(1 - \frac{q_t}{q_e}\right) = \frac{-K_1}{2.302}t \tag{6}$$

(3) Pseudo-second-order model:

$$\frac{t}{q_t} = \frac{t}{q_e} + \frac{1}{K_2 q_e^2} \tag{7}$$

(4) Intra-particle diffusion model :

$$q_t = K_i t^{0.5} + I \tag{8}$$

(5) Modified Freundlich model:

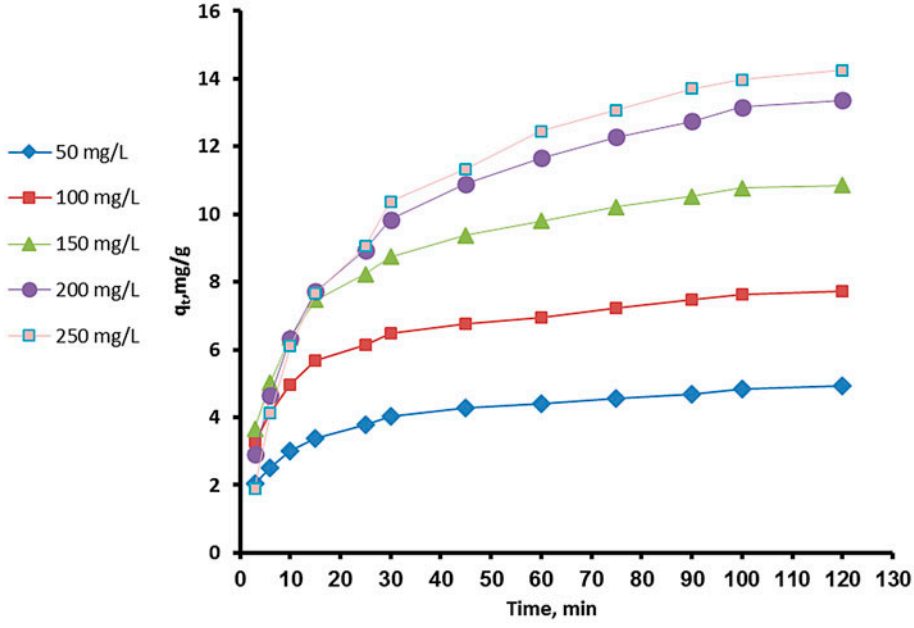

Fig. 5. Effect of contact time on phenol adsorption by CSP at different initial phenol concentrations.

$$\ln q_t = \ln(K_f C_0) + \frac{1}{m}\ln t \quad (9)$$

(6) Elovich model:

$$q_t = \left(\frac{\alpha}{\beta}\right)\ln(\alpha\beta) + \left(\frac{1}{\beta}\right)\ln t \quad (10)$$

where q_e (mg/g) and q_t (mg/g) are the amounts of phenol adsorbed by CSP at equilibrium and at different time intervals, respectively. k_1 (1/min) and k_2 (g/mg min) are the pseudo-first-order and pseudo-second-order rate constants, k_i is the intra-particle diffusion rate constant (mg/g $\text{min}^{0.5}$), k_f (1/g) and m are Freundlich constants, and α (mg/g min) and β (g/mg) are Elovich constants.

The linear plots [log $(1-q_t/q_e)$ vs. t], [t/q_t vs. t], [ln q_t vs. ln t], [q_t vs. $t^{0.5}$], and [q_t vs. ln t] allowed for checking the validity of different models. The kinetic parameters calculated from Eqs. (6)–(10). For the adsorption of different concentrations of phenol on CSP are given in Table 4. The pseudo-second-order model successfully fit the adsorption kinetic. According to Table 4, the pseudo-second-order seems to be the most appropriate one, owing to the highest recorded correlation coefficients (always above 0.99).

3.5. Response surface methodology

Prior knowledge and understanding of the process and the process variables under investigation are necessary for achieving a more realistic model. The range and level of variables that were used in this experimental design were decided on the basis of equilibrium and kinetic studies and also earlier reports [43]. Experimental data obtained for phenol removal are presented in Table 2. RSM was used to analyze the relationship between the variables and phenol removal efficiency. Fitting of the data to various models (linear, two-factor interaction, quadratic, and cubic) and their subsequent ANOVA showed that phenol removal was most suitably described with linear model. The predicted values for the response obtained from the model were sufficiently correlated to the observed values (Table 2).

Multiple regression coefficients of a second-order polynomial model describing the phenol removal are summarized in Table 5. F- and p-value were computed to determine the significance of each coefficient. Based on the p-values, A, B, C, B^2, AB, and BC were significant model terms. Other model terms (A^2, C^2, and AC) were not significant (with the probability value of larger than 0.05) and were thus eliminated. As observed in Table 5, the first order effects of CSP dosage, phenol concentration, and contact time, second-order effect of phenol concentration, and the two-factor interactions of CSP dosage, phenol concentration, and contact time produced the main effect on phenol removal efficiency. The following linear model describes the phenol removal efficiency as a function of the variables in terms of coded factors:

$$\text{Phenol Removal}\ (\%) = +55.03 + 6.34\text{A} + 4.46\text{B} - 27.45\text{C} - 8.51\text{D} + 4.19\text{CD} \quad (11)$$

Table 4
Kinetic model parameters for the adsorption phenol at different concentration on CSP

Kinetic model parameters	Kinetic parameters	Phenol concentration (mg/l)				
		50	100	150	200	250
Pseudo-first-order	K_1	0.025	0.0207	0.03	0.032	0.029
	r^2	0.974	0.973	0.985	0.977	0.992
Pseudo-second-order	K_2	0.0263	0.0184	0.01	0.0045	0.0031
	r^2	0.998	0.998	0.998	0.998	0.998
Modified Freundlich	M	4.37	4.54	3.62	2.58	2.05
	k_f	0.034	0.028	0.021	0.012	0.007
	r^2	0.972	0.954	0.948	0.952	0.915
Pore diffusion	K_i	0.288	0.435	0.716	1.078	1.27
	r^2	0.916	0.893	0.899	0.932	0.927
Elovich	A	3.67	7.16	4.83	3.27	5.84
	B	1.27	0.834	0.51	0.34	0.29
	r^2	0.994	0.995	0.991	0.992	0.996

Table 5
Estimated regression coefficients and corresponding to ANOVA results from the data of CCD experiments before elimination of insignificant model terms: (CSP)

Model terms	Coefficient estimate	Standard error	Sum of squares (SS)	Degree of freedom (DF)	Mean square (MS)	*F*-value	*p*-value	
Linear model			18,634.78	14	1,331.06	79.12	<0.0001	Significant
A	6.34	1.01	662.91	1	662.91	39.40	<0.0001	Significant
B	4.46	1.01	328.26	1	328.26	19.51	0.0005	Significant
C	−27.45	1.01	12,436.09	1	12,436.09	739.22	<0.0001	Significant
D	−8.51	1.01	1,196.21	1	1,196.21	71.10	<0.0001	Significant
A^2	−7.58	10.05	9.56	1	9.56	0.57	0.4627	Not significant
B^2	−3.82	10.05	2.43	1	2.43	0.14	0.7094	Not significant
C^2	−8.50	10.05	12.02	1	12.02	0.71	0.4113	Not significant
D^2	−3.12	10.05	1.62	1	1.62	0.096	0.7607	Not significant
AB	0.092	1.03	0.14	1	0.14	8.028E-003	0.9298	Not significant
AC	−0.89	1.03	12.76	1	12.76	0.76	0.3975	Not significant
AD	−0.77	1.03	9.56	1	9.56	0.57	0.4625	Not significant
BC	−1.01	1.03	16.42	1	16.42	0.98	0.3388	Not significant
BD	−0.53	1.03	4.55	1	4.55	0.27	0.6107	Not significant
CD	4.19	1.03	281.15	1	281.15	16.71	0.0010	Significant

ANOVA was used to test the significance of the fit of the model (Eq. (11)) under a wide range of operating conditions. The results are presented in Table 6 (numerically) and Fig. 6 (graphically). Data given in this table demonstrate that the linear model was significant at 5% confidence level, since p values (0.0001) were less than 0.05. On the basis of the calculated Fisher's F-test value (describing the variation of the data around the fitted model) and the corresponding probability values of 92.65 and <0.0001 (Table 5), it is concluded that this model can be characterized as highly significant in predicting phenol removal by CSP. Fitting of the model to the empirical data was tested by calculating determination coefficient (R^2). High value of R^2 (98%) designated the capability of the developed model to satisfactorily describe the system behavior within the investigated range of operating parameters. Adequate precision is a measure of the range in predicted phenol removal relative to its associated error; i.e. a signal-to-noise ratio. Its desired value is 4 or more. In this case, the ratio of 32.25 indicates an adequate signal. A very high degree of

Table 6
ANOVA for fit of phenol removal efficiency from CCD after elimination of insignificant model terms:(CSP)

Model	Significant model terms	SD	R^2	Adj. R^2	CV	Adeq. precision	PRESS	*p*-value	*F*-value	Probability for lack of fit
TCOD removal (%) Quadratic model	A, B, C, D, CD	4.1	0.986	0.974	7.45	32.25	1,051.64	0.0001	92.65	0.1438

Notes: R^2: determination coefficient, Adj. R^2: adjusted R^2, Adeq. precision: adequate precision, SD: standard deviation.
CV: coefficient of variation, PRESS: predicted residual error sum of squares.

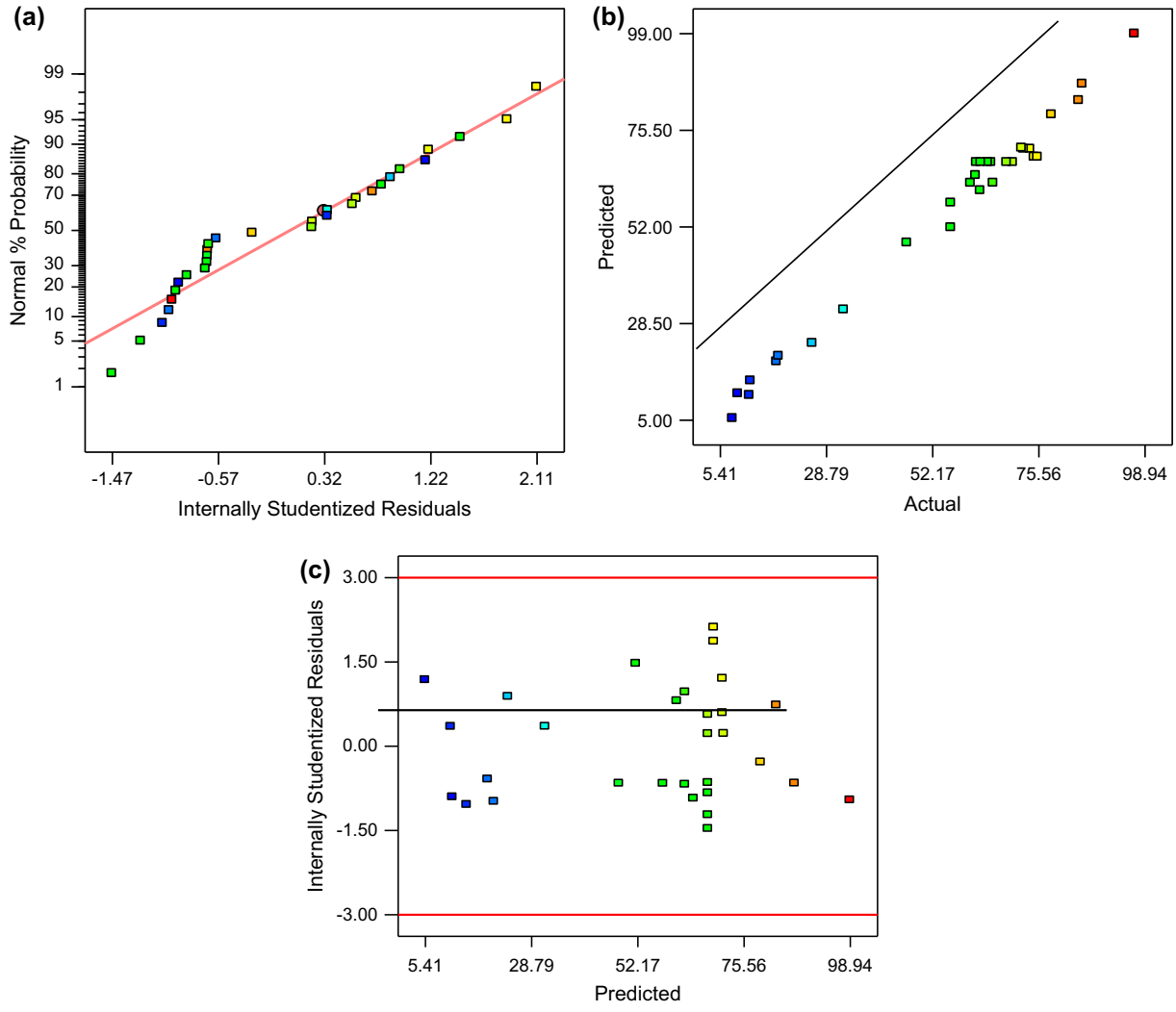

Fig. 6. (a) Normal probability plot of residual for phenol removal, (b) predicted vs. actual values plot for phenol removal, and (c) plot of residual vs. predicted response for phenol removal.

precision and a good deal of reliability of the experimental values were indicated by a low value of the coefficient of variation (CV = 7.45%).

Other important information on model performance can be found in the diagnostic plots (Fig. 6(a)–(c)), which provided a clear view in any deficiency of model fitting to the empirical data. Fig. 6(a) displays the normal probability of the residuals in order to verify whether the standard deviations between the actual and predicted response values followed a normal distribution [44]. Points and point clusters in normal probability plot were placed very close to the diagonal line (Fig. 6(a)), indicating that: (i) There are no violations in the assumptions that errors are normally distributed and independent from each other; (ii) error variances are homogeneous, and (iii) residuals are independent [45]. In Fig. 6(b), the values of R^2 and adjusted R^2 were evaluated as 0.986 and 0.974, respectively, showing a very good agreement between the predicted and actual data.

The plots of residual vs. predicted responses are illustrated in Fig. 6(c). It can be seen that all the points of experimental runs were randomly scattered and all values were within the range of −2.5 and 2.25 (values between −3 and +3 were considered as the top and bottom outlier detection limits), implying that the proposed models were adequate and that the constant variance assumption was confirmed.

To gain a better understanding of the interaction effects of variables affecting phenol removal efficiency, three-dimensional contour plots for the measured response were formed, based on the model (Eq. 2 and 11) shown in Fig. 7(a)–(c). Fig. 7(a) shows the

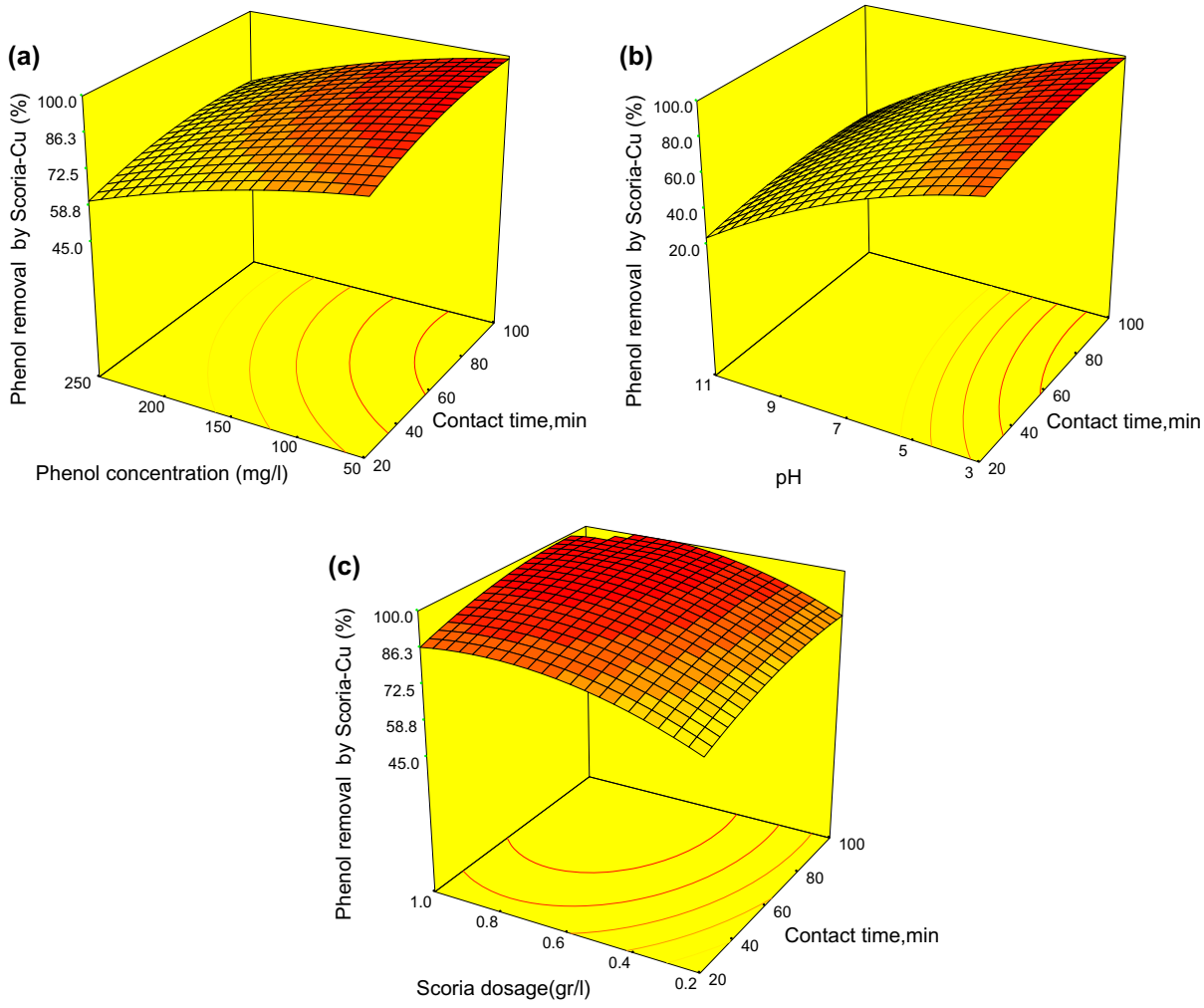

Fig. 7. Response surface plots for phenol removal efficiency with respect to (a) contact time and pH, (b) contact time and scoria dosage, and (c) contact time and phenol concentration.

response surface and contour plots for phenol removal efficiency as a function of initial phenol concentration and contact time for pH of 3 and adsorbant dosage of 1 g/l. It can be seen in Fig. 7(a) that the percentage of phenol removal decreased as the initial concentration of the phenol was increased. The percentage removal was gradually decreased from 98 to 30% as the phenol concentration increased from 50 to 250 mg/l, which can be explained in terms of the limited number of accessible active sites on the surface of adsorbent, which leads to a decrease in removal efficiency. The effects of pH and contact time on the phenol removal are shown in Fig. 7(b). The examination of the figure shows that the pH of the emulsion had a crucial effect on performance. A reverse impact of pH on COD removal was observed as the variable was increased (Fig. 7(b)), which can be attributed to the point that the solution pH can affect the surface charge of the adsorbent, degree of ionization of different pollutants, dissociation of functional groups on the active sites of the adsorbent, as well as structure of the dye molecule. Fig. 7(b) demonstrates that phenol adsorption on the surface of adsorbent decreased from 80 to 35% when the pH solution was increased from 3 to 11. The decrease in phenol removal under alkaline conditions may be due to the competition of excess of hydroxyl ions with phenoxide ions for active sites on the scoria powder. Effect of adsorbent dosage on phenol adsorption was studied in the range of 0.2–1 g/l under the conditions specified in Table 2. The results regarding phenol removal and adsorption capacity at various adsorbent doses are presented in Fig. 7(c). According to Fig. 7(c), increasing the adsorbent dosage from 0.2 to 1 g/l also increased percentage of phenol removal from 50 to 98%. The enhancement of phenol adsorption as a function of adsorbent dosage can be due to

Table 7
Numerical optimization for CCD

Number	A: Scoria dosage (g/l)	B: Contact time (min)	C: pH	D: Phenol concentration (mg/l)	Phenol removal by scoria-Cu %	Desirability	
Optimized phenol removal calculated from central composite design							
1	1	100	3	50	96.771	0.966	Selected
2	1	99	3	50	96.700	0.964	
3	1	100	3	50	96.217	0.963	
4	1	98	3	50	96.661	0.960	
5	1	100	3	50	96.700	0.958	
6	1	100	3	50	95.660	0.958	
7	1	100	3	65	96.700	0.956	
8	1	100	3	50	96.700	0.955	
9	1	100	3	72	96.700	0.951	
10	1	100	3	75	96.700	0.950	

Table 8
Confirmation between optimized phenol removals calculated from mathematical design and experimental study

Optimized phenol removal calculated from central composite design (predicted value)				
A: Scoria dosage (g/l)	B: Contact time (min)	C: pH	D: Phenol concentration (mg/l)	Phenol removal by scoria-Cu (%)
1	100	3	50	96.77
Confirmation study of optimized phenol removal (experimental value)				
1	100	3	50	96.7
$\text{Error}\,(\%) = \frac{\text{Actualvalue} - \text{Predictedvalue}}{\text{Actual value}} \times 100$				0.07%

the higher availability of active binding sites and the presence of a greater surface area for adsorption. The effect of contact time on phenol removal is presented in Figs. 7(a)–(c). These results indicated that the removal extent of phenol by adsorbent was increased with increasing contact time. The removal of phenol by adsorption on CSP was found to be rapid in the initial period of contact time end then became slow with the increase in contact time, which was caused by strong attractive forces between the phenol molecules and sorbent. Fast diffusion onto the external surface was followed by fast pore diffusion into the intraparticle matrix to attain rapid equilibrium.

3.6. Optimization and verification

The process optimization was performed by numerical optimization defined in Design Expert software. In the numerical optimization, the program sought to maximize desirability function for the optimum proposed condition. All four variables and phenol removal were set in the experimental ranges for maximum desirability. Using Table 7, it can be seen that the most desirable operating conditions were CSP dosage of 1 g/l, phenol concentration of 50 mg/l, and contact time of 100 min. This optimum operating condition with 0.98 desirability value was expected to be able to reach high phenol removal efficiency. In order to validate the optimum point generated by CCD, an experimental run was conducted at the CSP dosage of 1 g/l, phenol concentration of 50 mg/l, and contact time of 100 min. The validation results showed that experimental value (phenol removal: 96.77%) was found to be in good agreement with the value predicted from CCD (phenol removal: 96.7%) (Table 8). Errors between predicted and actual values were 0.07%, showing that process optimization in CCD was able and reliable in terms of modeling and optimizing phenol adsorption by CSP.

4. Conclusion

CSP has been found to be an effective adsorbent for the removal of phenol from an aqueous solution.

Also, the present study demonstrates the use of a CCD in term of determining the conditions which leads to high phenol removal efficiency. Optimum conditions for phenol removal were achieved with RSM under Design Expert software at 1 g/l of CSP dose, initial phenol concentration of 50 mg/l, contact time of 100 min, and pH of 3. The results indicated that the CSP is efficient (96%) in removal of phenol from the aqueous solution in the optimum conditions. The Langmuir adsorption isotherm fitted well with the equilibrium adsorption data. This adsorption process obeyed a pseudo-second-order kinetics rate model. It can be concluded that the CSP could be used as a low-cost, natural, and abundant source for the removal of phenol from wastewater and it might be utilized as an alternative of more costly methods such as activated carbon adsorption.

References

[1] K. Saravanakumar, A. Kumar, Removal of phenol from aqueous solution by adsorption using zeolite, Afri. J. Agric. Res. 8(23) (2013) 2965–2969.

[2] S.M. Mousavi, I. Alemzadeh, M. Vossoughi, Use of modified bentonite for phenolic adsorption in treatment of olive oil mill wastewater, Iran. J. Sci. Tech. Trans. B Eng. 30 (2006) 613–619.

[3] S. Al-Asheh, F. Banat, L. Abu-Aitah, Adsorption of phenol using different types of activated bentonites, Sep. Purif. Technol. 33 (2003) 1–10.

[4] R.I. Yousef, B. El-Eswed, A.H. Al-Muhtaseb, Adsorption characteristics of natural zeolites as solid adsorbents for phenol removal from aqueous solutions: Kinetics, mechanism, and thermodynamics studies, Chem. Eng. J. 171(3) (2011) 1143–1149.

[5] F.A. Banat, B. Al-Bashir, S. Al-Asheh, O. Hayajneh, Adsorption of phenol by bentonite, J. Environ. Pollut. 107(3) (2000) 391–398.

[6] Institute of Standards and Industrial Research of Iran, Quality Standards of Drinking Water, Tehran, ISIRI, 1997, p. 1053 (in Persian).

[7] B. Ozkaya, Adsorption and desorption of phenol on activated carbon and a comparison of isotherm models, J. Hazard. Mater. 129(1–3) (2006) 158–163.

[8] B. Koubaissy, G. Joly, P. Magnoux, Adsorption and competitive adsorption on zeolites of nitrophenol compounds present in wastewater, Indian Eng. Chem. Res. 47(23) (2008) 9558–9565.

[9] M. Carbajo, F.J. Beltran, F. Medina, O. Gimeno, F.J. Rivas, Catalytic ozonation of phenolic compounds: The case of gallic acid, Appl. Catal., B 67(3–4) (2006) 177–186.

[10] A. Quintanilla, J.A. Casas, A.F. Mohedano, J.J. Rodriguez, Reaction pathway of the catalytic wet air oxidation of phenol with a Fe/activated carbon catalyst, Appl. Catal., B 67(3–4) (2006) 206–216.

[11] S. Esplugas, J. Giménez, S. Contreras, E. Pascual, M. Rodríguez, Comparison of different advanced oxidation processes for phenol degradation, Water Res. 36(4) (2002) 1034–1042.

[12] J.A. Zazo, J.A. Casas, A.F. Mohedano, J.J. Rodríguez, Catalytic wet peroxide oxidation of phenol with a Fe/active carbon catalyst, Appl. Catal., B 65(3–4) (2006) 261–268.

[13] A.P. Annachhatre, S.H. Gheewala, Biodegradation of chlorinated phenolic compounds, Biotechnol. Adv. 14 (1) (1996) 35–56.

[14] Z. Guo, R. Ma, G. Li, Degradation of phenol by nanomaterial TiO_2 in wastewater, Chem. Eng. J. 119(1) (2006) 55–59.

[15] A. Tor, Y. Cengeloglu, M.E. Aydin, M. Ersoz, Removal of phenol from aqueous phase by using neutralized red mud, J. Colloid Interface Sci. 300(2) (2006) 498–503.

[16] M.R. Panuccio, A. Sorgonà, M. Rizzo, G. Cacco, Cadmium adsorption on vermiculite, zeolite and pumice: Batch experimental studies, J. Environ. Manage. 90(1) (2009) 364–374.

[17] S.S. Kaplan Bekaroglu, N.O. Yigit, T. Karanfil, M. Kitis, The adsorptive removal of disinfection byproduct precursors in a high-SUVA water using iron oxide-coated pumice and volcanic slag particles, J. Hazard. Mater. 183(1–3) (2010) 389–394.

[18] N. Moraci, P.S. Calabrò, Heavy metals removal and hydraulic performance in zero-valent iron/pumice permeable reactive barriers, J. Environ. Manage. 91(11) (2010) 2336–2341.

[19] B. Ozturk, Y. Yildirim, Investigation of sorption capacity of pumice for SO_2 capture, Process Saf. Environ. Prot. 86(1) (2008) 31–36.

[20] M.R. Samarghandi, M. Zarrabi, M.N. Sepehr, A. Amrane, G.H. Safari, S. Bashiri, Application of acidic pumice as an adsorbent the removal of azo dye from aqueous solutions: Kinetic, equilibrium and thermodynamic studies, Iran. J. Environ. Health Sci. Eng. 99(1) (2012) 33–44.

[21] M. Heidari, F. Moattar, S. Naseri, M.T. Samadi, N. Khorasani, Evaluation of aluminum-coated pumice as a potential arsenic (V) adsorbent from water resources, Int. J. Environ. Res. 5(2) (2011) 447–456.

[22] D. Baş, İ.H. Boyacı, Modeling and optimization I: Usability of response surface methodology, J. Food Eng. 78(3) (2007) 836–845.

[23] G.E.P. Box, N.R. Draper, Empirical Model-building and Response Surfaces, Wiley, New York, NY, 1987.

[24] A.L. Ahmad, S. Ismail, S. Bhatia, Optimization of coagulation–flocculation process for palm oil mill effluent using response surface methodology, Environ. Sci. Technol. 39(8) (2005) 2828–2834.

[25] A. Azizi, M.R. Alavi Moghaddam, M. Arami, Application of wood waste for removal of reactive blue 19 from aqueous solutions: Optimization through response surface methodology, Environ. Eng. Manage. J. 11(4) (2012) 795–804.

[26] F. Shahrezaei, Y. Mansouri, A.A. Zinatizadeh, Process modeling and kinetic evaluation of petroleum refinery wastewater treatment in a photocatalytic reactor using TiO_2 nanoparticles, Powder Technol. 221 (2012) 203–212.

[27] M. Shirzad-Siboni, S.J. Jafari, M. Farrokhi, J.K. Yang, Removal of phenol from aqueous solutions by activated red mud: Equilibrium and kinetics studies, Environ. Eng. Res. 18(4) (2013) 247–252.

[28] A.I. Khuri, J.A. Cornell, Response Surfaces: Design and Analyses, second ed., Marcel Dekker, New York, NY, 1996.
[29] B. Ersoy, A. Sariisik, S. Dikmen, G. Sariisik, Characterization of acidic pumice and determination of its electrokinetic properties in water, Powder Techol. 197 (1–2) (2010) 129–135.
[30] D.C. Montgomery, Design and Analysis of Experiments, third ed., Wiley, New York, NY, 1991.
[31] R.L. Mason, R.F. Gunst, J.L. Hess, Statistical Design and Analysis of Experiments, Eighth Applications to Engineering and Science, second ed., Wiley, New York, NY, 2003.
[32] R. Grim, Clay Mineralogy, McGraw-Hill Book Company, New York, NY, 1968, p. 596.
[33] M. Kitis, E. Karakaya, N.O. Yigit, G. Civelekoglu, A. Akcil, Heterogeneous catalytic degradation of cyanide using copper-impregnated pumice and hydrogen peroxide, J. Water Res. 39(8) (2005) 1652–1662.
[34] N. Dizge, B. Keskinler, H. Barlas, Sorption of Ni(II) ions from aqueous solution by Lewatit cation-exchange resin, J. Hazard. Mater. 167(1–3) (2009) 915–926.
[35] A. Sarı, M. Tuzen, Kinetic and equilibrium studies of biosorption of Pb(II) and Cd(II) from aqueous solution by macrofungus (*Amanita rubescens*) biomass, J. Hazard. Mater. 164(2–3) (2009) 1004–1011.
[36] F.N. Arslanogˇlu, F. Kar, N. Arslan, Adsorption of dark coloured compounds from peach pulp by using powdered-activated carbon, J. Food Eng. 71(2) (2005) 156–163.
[37] T.W. Weber, R.K. Chakravorti, Pore and solid diffusion models for fixed-bed adsorbers, Amer. Institute Chem. Eng. J. 20(2) (1974) 228–238.
[38] S. Veli, B. Alyüz, Adsorption of copper and zinc from aqueous solutions by using natural clay, J. Hazard. Mater. 149(1) (2007) 226–233.
[39] A. Arslan, S. Veli, Zeolite 13X for adsorption of ammonium ions from aqueous solutions and hen slaughterhouse wastewaters, J. Taiwan Inst. Chem. Eng. 43(3) (2012) 393–398.
[40] A. Mittal, D. Kaur, A. Malviya, J. Mittal, V.K. Gupta, Adsorption studies on the removal of coloring agent phenol red from wastewater using waste materials as adsorbents, J. Colloid Interface Sci. 337 (2009) 345–354.
[41] T.K. Naiya, A.K. Bhattacharya, S.K. Das, Adsorption of Cd(II) and Pb(II) from aqueous solutions on activated alumina, J. Colloid Interface Sci. 333(1) (2009) 14–26.
[42] J. Febrianto, A.N. Kosasih, J. Sunarso, Y.-H. Ju, N. Indraswati. Equilibrium and kinetic studies in adsorption of heavy metals using biosorbent: A summary of recent studies, J. Hazard. Mater 162(2–3) (2009) 616–645.
[43] F. Akbal, Adsorption of basic dyes from aqueous solution onto pumice powder, J. Colloid Interface Sci. 286 (2) (2005) 455–458.
[44] K.M. Lee, D.F. Gilmore, Modeling and optimization of biopolymer (polyhydroxyalkanoates) production from ice cream residue by novel statistical experimental design, Appl. Biochem. Biotechnol. 133(2) (2006) 113–148.
[45] H. Kusic, N. Koprivanac, A.L. Bozic, Treatment of chlorophenols in water matrix by UV/ferrioxalate system: Part I. Key process parameter evaluation by response surface methodology, Desalin.Water Treat. 280(1–3) (2011) 208–216.